Inorganic Chemistry
Article
pubs.acs.org/IC

A Trigonal Prismatic Ligand in the Metal-Mediated Self-Assembly of One- and Two-Dimensional Metallosupramolecular Polymers

Wen-Jing Hu,[†] Long-Qing Liu,[‡] Ming-Liang Ma,*[,‡] Xiao-Li Zhao,[§] Yahu A. Liu,[¶] Xian-Qiang Mi,[†] Biao Jiang,*[,†] and Ke Wen*[,†,‡]

[†]Sustainable Technology Research Center, Shanghai Advanced Research Institute, Chinese Academy of Science, Shanghai 201210, China

[‡]Shanghai Engineering Research Center of Molecular Therapeutics and New Drug Development, East China Normal University, Shanghai 200062, China

[§]Shanghai Key Laboratory of Green Chemistry and Chemical Processes, and Department of Chemistry, East China Normal University, Shanghai 200062, China

[¶]Medicinal Chemistry, ChemBridge Research Laboratories Inc., San Diego, California 92127, United States

Supporting Information

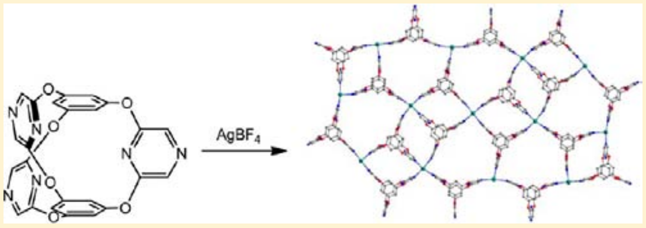

ABSTRACT: A novel trispyrazine-pillared prismatic bicyclooxacalixaromatic ligand **L** is synthesized, and its application in metal-mediated self-assembly is described. Under self-assembly conditions, single chain, double-stranded cross-linked coordination polymer and two-dimensional (2D) coordination polymeric networks were formed via **M-L** (Ag^+, Cu^{2+}, and Zn^{2+}) coordinative interactions. Structural analyses revealed that the antiparallelly arranged one-dimensional coordination polymers (Cu^{2+} and Zn^{2+}) are arranged to generate well-defined voids to host aromatic guests (benzene) via C−H···π and π···π interactions, while the double-stranded cross-linked coordination polymer (Ag^+) contains a rhomboidal $[\mathbf{Ag_2(L^3)_2}]$ ($\mathbf{L^3}$: tridentate ligand) cage motif to include a benzene guest; the "thicker" (thickness: *ac* 5 Å) 2D coordination polymeric networks (Ag^+, Cu^{2+}, and Zn^{2+}), however, are all formed by connection of one or two kinds of topologically different metallomacrocyclic cage units. These unique metallomacrocyclic cage units in the 2D coordination polymeric networks are capable of hosting different guest species. For instance, the rhomboidal $[\mathbf{M_2(L^3)_2}]$ (M = Ag^+, Cu^{2+}) cage units were found to host a benzene or a nitrate anion; a hexahedral $[\mathbf{M_3(L^3)_3}]$ (M = Ag^+) cage was found to host a ligand **L** or a DMF molecule; the hexahedral $[\mathbf{M_4(L^3)_4}]$ (M = Cu^{2+}) cage was found to host four solvent molecules of benzene; and the rectangular $[\mathbf{M_3(L^3)_3}]$ (M = Cu^{2+}, Zn^{2+}) cage units, however, were found to host two THF molecules. The results highlight the potential of ligand **L** for applications in the construction of "thicker" 2D coordination polymeric networks with well-defined metallomacrocyclic cage units capable of hosting various guest species.

■ INTRODUCTION

Metal-mediated self-assembly is an increasingly versatile and attractive approach for the construction of aesthetically appealing supramolecular architectures[1] and functional metal−organic discrete assemblies and polymeric networks for applications in molecular recognition and separation,[2] catalysis,[3] storage,[4] stabilization of reactive speciesm and controlling chemical transformations.[5] It is well-known that the ligating topologies of the organic ligands used in the metal-mediated self-assembly play a key role in determining the structural and functional properties of the resultant metallosupramolecular objects. Much efforts have therefore been devoted to rationalize the ligand design for controlling the geometries and functionalities of the resulting metal−ligand assemblies.[6−10] Conformational well-defined macrocyclic compounds, such as calixarenes, resorcinarenes, and cyclotriveratrylenes, have been playing a very important role in host−guest chemistry.[11,12] The integration of metal binding sites into these macrocyclic compounds led to macrocyclic ligands that have been successfully used in the metal-mediated self-assembly of nanosized coordination cages,[13−15] interlocking catenating assemblies,[16] and "Solomon cube".[17] Previously, we[18] and others[19] have succeeded in the synthesis of heteracalixaromatics,[20] with *exo*-nitrogen-heterocyclic termini, and the investigation of the coordination-driven self-assembly based on these heteracalixaromatic ligands led to the generation of metallomacrocyclic cages and coordination polymers.[21] Recently, heterabicyclooxacalixaromatics,[22] conformationally restricted analogues of heteracalixaromatics with a trigonal prismatic cage-like structure of high symmetry have been synthesized. We envisioned that integration of metal binding sites into this trigonal prismatic scaffold would create a three-dimensional ligand,[23] topologically different from those of

Received: March 28, 2013
Published: August 8, 2013

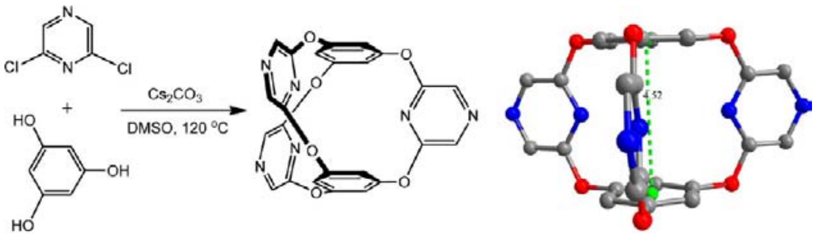

Figure 1. Synthesis and structure of the three-dimensional trigonal prismatic ligand **L**. Hydrogen atoms are omitted for clarity. Color code: O (red), N (blue), C (gray).

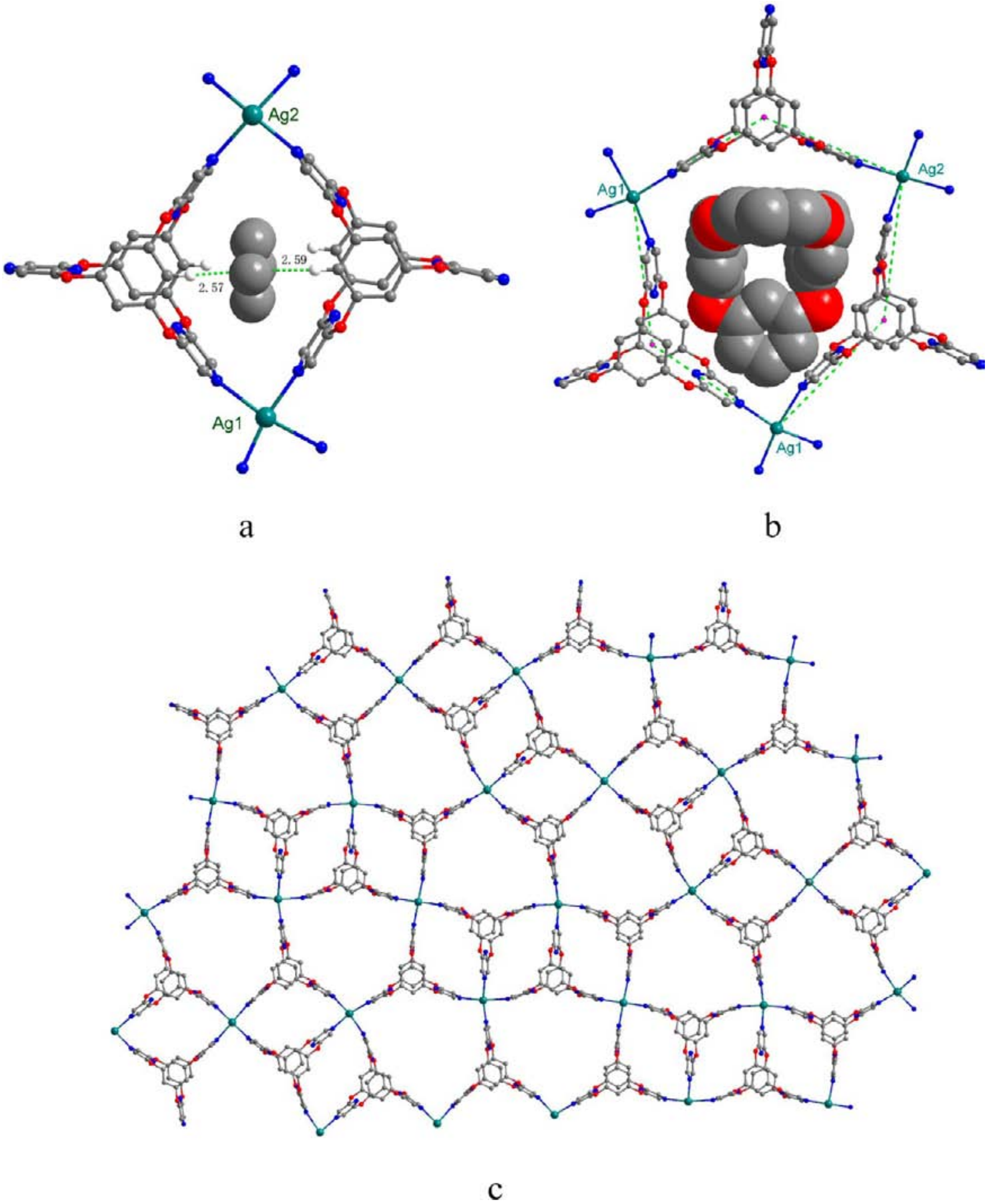

Figure 2. The [**$Ag_2(L^3)_2$·benzene**] rhomboidal (a) and [**$Ag_3(L^3)_3$·L**] hexagonal (b) cage motifs in **1** with guest species of benzene and ligand **L** being included, respectively, and the overall 2D polymeric network structure of complex **1** (c). BF_4^- anions, hydrogen atoms, and guest species included in the cage units in c are omitted for clarity. Color code: Ag (purple), O (red), N (blue), C (gray), H (white).

traditional triangular "planar" ligands,[24] and the application of such a three-dimensional ligand in the metal-mediated self-assembly presents an opportunity to construct novel cavity containing metallosupramolecular architectures. Herein, we report on the synthesis of a bicyclooxacalix[2]benzene[3]-pyrazine **L** (Figure 1), a novel cagelike trigonal pyrazinyl-pillared prismatic ligand, and its application in metal-mediated self-assembly of various one- and two-dimensional (1D and 2D) coordination supramolecular polymers under different reaction conditions (counteranions, solvent systems used). One crucial feature for the structure of **L** is that its three ligating planes (pyrazinyl rings) lie orthogonally to the two centered parallel phenyl planes with the dihedral angles close to 120°. In the 2D coordination self-assembled metallosupramolecular networks, the ligand−metal−ligand bridges result in various metallomacrocyclic cage units with confined interior cavities generated by the concave surfaces of **L**. Small neutral and charged guest species were found to be included in these metallomacrocyclic cages.

RESULTS AND DISCUSSION

Synthesis and Structure of Bicyclo-oxacalix[2]-benzene[3]pyrazine L. The three-dimensional trigonal prismatic ligand **L** was synthesized in 15% yield by direct heating of phloroglucinol and 2,6-dichloropyrazine at 120 °C in DMSO for 12 h in the presence of Cs_2CO_3, similar to the synthesis of other bicyclooxacalixaromatics.[22a] **L** was fully characterized by ^{1}H and ^{13}C NMR (Supporting Information), ESI-MS spectra and single-crystal X-ray diffraction analysis. As shown in Figure 1, ligand **L** adopts a highly symmetrical, double-decker, all-1,3-alternate cagelike structure, where the two benzene planes as the decks are eclipsing and cofacially separated by 4.52 Å. The two benzene rings and the three pillared pyrazine planes are arranged almost orthogonal (the dihedral angles between the two benzene rings and the pillared pyrazine planes are around 87−90°). The six nitrogen atoms of the three pyrazinyl pillars are located in one plane which is parallel to the two benzene ring planes. The dihedral angles between the three pyrazinyl ring planes are close to 120°. Compared to 2,4,6-tris(4-pyridyl)-1,3,5-triazine (tpt),[1c,23] a traditional triangular "planar" ligand, the three-dimensional trigonal prismatic ligand **L** possesses the following unique characteristics: (1) the three pyrazinyl planes lie orthogonally to the central nitrogen plane and generate six concave surfaces that could interact with potential guest molecules more efficiently; (2) upon coordination, the "walls" generated by the concave surfaces of **L** could produce larger voids for hosting guest molecules; (3) the ligating angles between the three pyrazinyl termini can be adjusted to fulfill the coordination environments adopted by different metal cations, thus increasing the diversity of the resulting coordinative self-assembled supramolecular architectures.

Silver-Mediated Self-Assembly of L and the Structures of the Resulting Supramolecular Complexes (1−3). **L** reacted with $AgBF_4$ in a mixed solvent of benzene and acetonitrile (ACN) to afford a 2D coordination polymer **1** (Supporting Information). Single crystals of **1** suitable for X-ray analysis were obtained by slow evaporation of the solvent at ambient temperature either in open air or in DMF atmosphere. ^{1}H NMR spectrum of **1** in solvents such as DMSO-d_6, CD_3CN, DMF-d_7, and CD_3OD, showed no proton shifts compared to the corresponding free ligand **L**, suggesting that complex **1** does not survive in these coordinating solvents. However, the ^{1}H NMR spectrum of **1** in CD_3NO_2 shows two sharp pyrazinyl proton signals, one corresponding to the pyrazinyl protons of free ligand **L** (no shift), while the other corresponding to the pyrazinyl protons of metal complexes (shift downfield by 0.58 ppm), suggesting some complex species $[Ag_nL_m]^{n+}$ exist in CD_3NO_2, and these species are under fast equilibration on the NMR time scale (Figure S1, Supporting Information). ESI-MS results show peaks at *m/z* 586.98 and 755.34 for **1** in acetonitrile solution, which are assigned to the 1:1 complex species of $[Ag(\mathbf{L})]^+$ and $[Ag(\mathbf{L})(ACN)_2\cdot(BF_4)]$ (Figure S2). The combined ^{1}H NMR and ESI-MS results suggest that the silver complex species of **L** polymerize upon crystallization to generate the two-dimensional coordination polymer **1**.[15b,21]

Because of the quality of the X-ray diffraction data of the single crystals of **1** obtained in benzene and acetonitrile, we were not able to obtain high-quality refinement, but the data could be used to determine the basic skeleton of **1**. Structural analysis revealed that **1** exhibits a 2D polymeric structure with a 4:3 stoichiometry between ligand **L** and Ag^+ ion, the polymeric structure is composed of two kinds of metallomacrocyclic cage motifs, namely, $[\mathbf{Ag_2(L^3)_2}]$ rhomboidal and $[\mathbf{Ag_3(L^3)_3}]$ hexagonal cage motifs ($\mathbf{L^3}$: tridentate ligand). As shown in Figure 2, the $[\mathbf{Ag_2(L^3)_2}]$ rhomboidal cage is formed by bridging two ligands **L** by two Ag^+ cations (Figures 2a and S3a), and analogously, the $[\mathbf{Ag_3(L^3)_3}]$ hexagonal cage is formed by connecting three ligands **L** by three Ag^+ cations, respectively, via Ag−N bonds (Figure 2b). Two crystallographically independent Ag^+ centers (**Ag1** and **Ag2**) are present in the polymeric complex **1**. Each Ag^+ center (**Ag1** and **Ag2**) is coordinated by four *exo*-pyrazinyl nitrogen atoms from four ligands **L** with the four Ag−N bonds (2.29−2.61 Å for **Ag1**, 2.36−2.50 Å for **Ag2**) forming a tetragonal plane (square-planar metal complex). The variation in Ag−N bond lengths and N−Ag−N angles (83.0−103.0° for **Ag1**, 86.7−91.9° for **Ag2**) indicates the distortion of the square-planar geometry of the Ag centers. The dihedral angles between the three pyrazinyl binding vectors in **L** were adjusted in **1** to accommodate the coordination geometry of the silver centers. In complex **1**, two different $[\mathbf{Ag_2(L^3)_2}]$ rhomboidal cage motifs exist; one is formed by **Ag1** and **Ag2** bridged by two **L** with **Ag1···Ag2** separation of 12.52 Å and N−Ag1−N and N−Ag2−N bond angles of 87.5° and 91.9°, respectively. The other is formed by two **Ag1** cations connected by two **L** with **Ag1···Ag1** separated by 12.82 Å, and two N−Ag1−N bond angles of 83.0° (Figure S3a). The $[\mathbf{Ag_2(L^3)_2}]$ rhomboidal cages are found to host a guest molecule of benzene via C−H···π interactions (Figures 2a and S3a). In the distorted $[\mathbf{(Ag1)_2(Ag2)(L^3)_3}]$ hexagonal cage motif, the three silver centers are separated by 13.91 Å, 14.18 Å, and 14.88 Å, with the three N−Ag−N bond angles (N−Ag1−N, N−Ag2−N, and N−Ag1−N) of 85.8°, 86.7°, and 103.0°, respectively (Figure S3b). The void of the $[\mathbf{Ag_3(L^3)_3}]$ cage unit is sufficiently large to host a small guest molecule but not large enough to host an entire ligand **L**, as only part of a ligand **L** is included (due to the quality of the data sets, the guest molecule **L** could not be fully determined), as shown in Figure 2b. The Ag^+ centers (**Ag1** and **Ag2**) are coordinatively saturated but allow electrostatic interactions of BF_4^- anions close to their apical positions to reach charge neutralization. The polymeric complex **1** stacks in a layered fashion that one layer sits above the other. Hence, 1D rhomboidal and hexagonal channels are formed along the *c*-axis by the stacked layers of **1**, and guest molecules of benzenes and ligands **L** are filled in the 1D rhomboidal and hexagonal channels, respectively (Figure S3c).

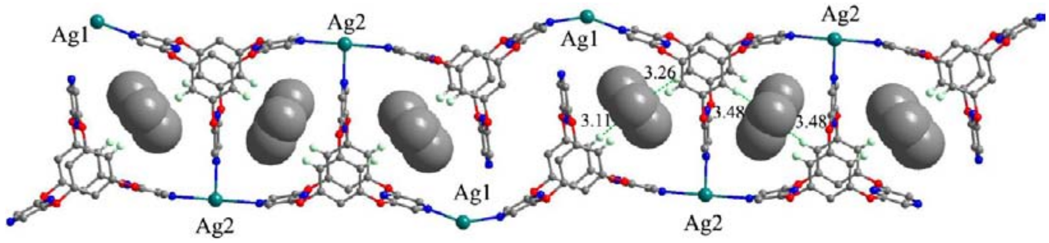

Figure 3. The structure of the antiparallel cross-linked double-stranded coordination polymer **2** with the benzene guests being included in the $\mathbf{Ag_2(L^3)_2}$ cage and the $\mathbf{Ag(L^2)(L^3)}$ uncapped cage-like units. Nitrate anions and hydrogen atoms other than those involved in hydrogen-bonding are omitted for clarity. Color code: Ag (purple), O (red), N (blue), C (gray), H (white).

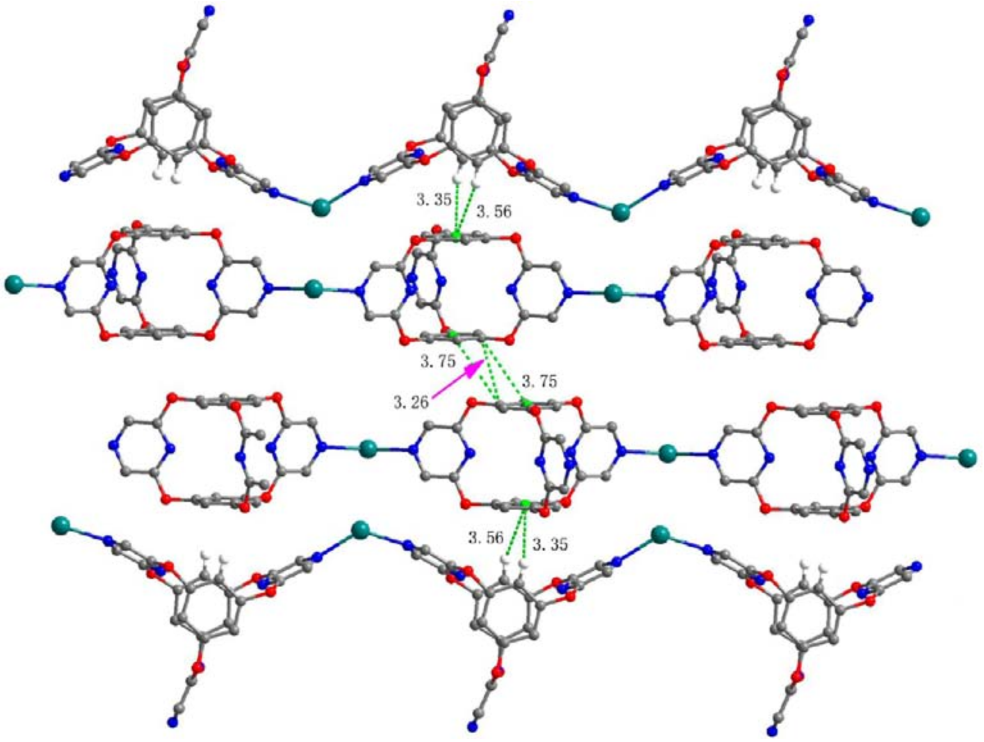

Figure 4. The molecular arrangement in a single layer of the polymer complex **3**. Nitrate anions, DMFs, and hydrogen atoms other than those involved in hydrogen-bonding are omitted for clarity. Color code: Ag (purple), O (red), N (blue), C (gray), H (white).

For the crystals of **1** obtained in the mixed solvent of benzene and acetonitrile under DMF atmosphere, the 1D $[\mathbf{Ag_3(L^3)_3}]$ hexagonal channels are no longer filled by ligands **L**; instead, they are filled by DMF molecules (Figure S4). This was the result of the replacement of ligands **L** by DMF molecules (diffused from the DMF atmosphere into the sample solution) in the crystallization process.

The reaction of **L** with $AgNO_3$ was carried out in two solvent systems: (1) benzene and acetonitrile, (2) acetonitrile and THF. Single crystals of silver complex **2** suitable for X-ray analysis were obtained by slow evaporation of the mixed solvent of benzene and acetonitrile at ambient temperature, while single crystals of silver complex **3** suitable for X-ray analysis were obtained by slow evaporation of a mixed solvent of THF and acetonitrile at ambient temperature under DMF atmosphere (for details, see Results and Discussion). Similar to complex **1**, complexes **2** and **3** do not survive in coordinating solvents such as DMSO-d_6, CD_3CN, DMF-d_7, and CD_3OD, as evidenced by no proton shifts being observed compared to the corresponding free ligand **L** in their ^1H NMR spectra in these solvents. The downfield shifts of the pyrazinyl proton signals (0.43 ppm) in the ^1H NMR spectrum of **2** in CD_3NO_2 indicate the existence of coordinative interaction between **L** and Ag^+ cation in CD_3NO_2 (Figure S5), while no shifts were observed in the ^1H NMR spectrum of **3** in CD_3NO_2, possibly being caused by the existence of coordinating DMF molecules in **3**. ESI-MS results show peaks at m/z 796.37 for complex **2** dissolved in acetonitrile (ACN), which is assigned to $[\mathbf{Ag_2(L)}(ACN).NO_3]^+$ (Figure S6a). While peaks at m/z 586.98 and 769.34 in the ESI-MS spectrum of complex **3** dissolved in acetonitrile are assigned to $[\mathbf{Ag(L)}]^+$ and $[\mathbf{KAg(L)}(ACN)_2{\cdot}NO_3]^+$ (Figure S6b), respectively. The ESI-MS results indicate the presence of silver complexes in solution and suggest that these complexes polymerize upon crystallization to generate silver complexes **2** and **3**.

Single crystal X-ray diffraction analysis established complex **2** as an antiparallel cross-linked double-stranded 1D coordination polymer containing $\mathbf{Ag_2(L^3)_2}$ cage and uncapped $\mathbf{Ag_2(L^2)(L^3)}$ cagelike units, as shown in Figure 3. In complex **2**, **L** acts as both bidentate ($\mathbf{L^2}$) and tridentate ($\mathbf{L^3}$) ligands to interact with Ag^+ cations. $\mathbf{L^2}$ and $\mathbf{L^3}$ are arranged alternately along a double-stranded polymeric chain with a **L**:Ag^+ ratio of 1:1. There are

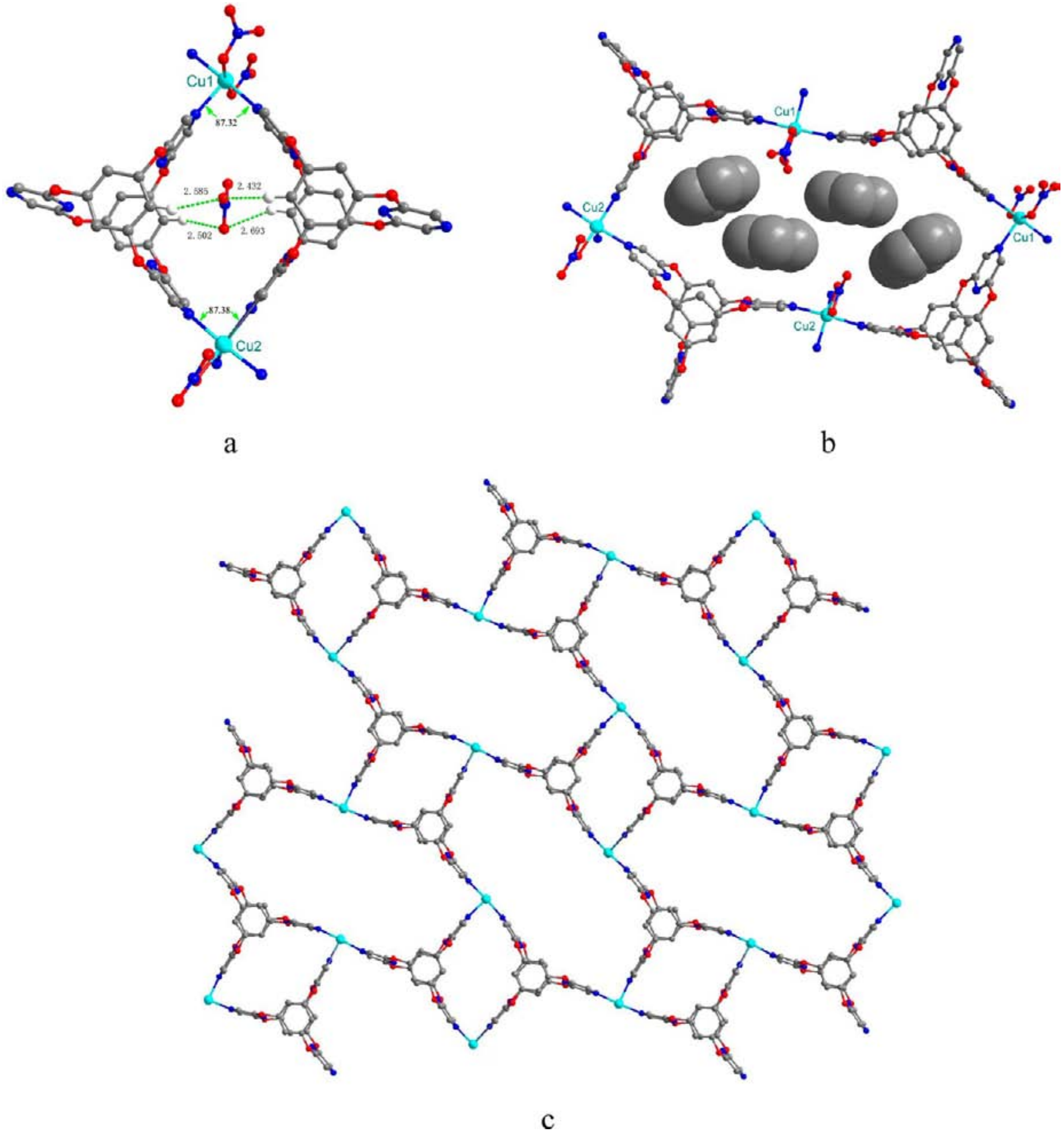

Figure 5. The rhomboidal $[\mathbf{Cu_2(L^3)_2}]$ (a) and $[\mathbf{Cu_4(L^3)_4 \cdot 4benzene}]$ hexagonal (b) cage motifs in **4** with guest species of nitrate and benzenes being included, respectively, and the overall 2D polymeric network structure of complex **4** (c). Hydrogen atoms other than those involved in hydrogen-bonding in a, nitrate anions, acetonitrile, and guest species included in the cage units in c are omitted for clarity. Color code: Cu (green), O (red), N (blue), C (gray), H (white).

two crystallographically nonequivalent silver coordination spheres **Ag1** and **Ag2** present in **2**. **Ag1** is found to adopt a distorted trigonal pyramidal arrangement and is occupied by two nitrogen atoms (Ag−N distances: 2.23 Å, 2.26 Å) from one $\mathbf{L^2}$ and one $\mathbf{L^3}$, and two oxygen atoms (Ag−O distances: 2.46 Å, 2.68 Å) from two coordinated nitrate counteranions (Figure S7a), while **Ag2** is found to adopt a highly distorted octahedral arrangement and is occupied by three nitrogen atoms (Ag−N distances, 2.34−2.64 Å) from one $\mathbf{L^2}$ and two $\mathbf{L^3}$, and three oxygen atoms (Ag−O distances, 2.46−2.74 Å) from two nitrate counteranions (Figure S7b). As a result, the three oxygen atoms and one nitrogen atom form a distorted tetragonal plane, and the remaining two nitrogen atoms occupy the two apical positions of the bipyramidal with an N−Ag−N bond angle of 173.97°. In the polymeric chain, **Ag1** and **Ag2** are connected by $\mathbf{L^2}$ and $\mathbf{L^3}$ alternately with two **Ag1**−**Ag2** distances of 14.66 Å and 14.86 Å, respectively. The two antiparallel coordinative polymeric chains are cross-linked by $\mathbf{L^3}$ via Ag−N bonds and resulted in the formation of $[(\mathbf{Ag2})_2(\mathbf{L^3})_2]$ rhomboidal cage and uncapped $[(\mathbf{Ag1})(\mathbf{Ag2})(\mathbf{L^2})(\mathbf{L^3})]$ cagelike structural units. The rhomboidal cage $[(\mathbf{Ag2})_2(\mathbf{L^3})_2]$ unit is highly symmetrical with the $\mathbf{Ag_2 \cdots Ag_2}$ separation of 12.30 Å and the two N−Ag−N angles of 92.5°. The uncapped $[(\mathbf{Ag1})(\mathbf{Ag2})(\mathbf{L^2})(\mathbf{L^3})]$ cagelike unit is topologically similar to that of the $[(\mathbf{Ag2})_2(\mathbf{L^3})_2]$ rhomboidal cage one but failed in the cross-connection of the free *exo*-nitrogen atom of $\mathbf{L^2}$ and **Ag1**. Both $[(\mathbf{Ag2})_2(\mathbf{L^3})_2]$ and $[(\mathbf{Ag1})(\mathbf{Ag2})(\mathbf{L^2})(\mathbf{L^3})]$ units in the double-stranded coordination polymer **2** act as molecular hosts to encapsulate a guest molecule of benzene via C−H···π interaction (Figure 3), similar to that of the [$\mathbf{Ag_2(L^3)_2}$] rhomboidal cage in complex **1**. In the solid state, the double-stranded polymeric chains of **2** are interconnected by nitrate anions via Ag−O bonds, and in this aspect, complex **2** is a three-dimensional network (Figure S7c).

Single crystal X-ray structure of **3**, determined at 173 K, revealed an infinite 1D polymeric topology with a 1:1 stoichiometry between bidentate ligand $\mathbf{L^2}$ and Ag^+ ion. No [$\mathbf{Ag_m(L^2)_n}$] cage units, such as those in **1** and **2**, were formed. As shown in Figure 4, the coordination polymer **3** is formed by an alternative connection of the bidentate ligand $\mathbf{L^2}$ and Ag^+ ion with the two coordinated pyrazine rings in each bidentate ligand $\mathbf{L^2}$ creating a "groove" along the polymeric chain. All Ag^+ centers are crystallographically equivalent and adopt a distorted trigonal bipyramidal arrangement occupied by two nitrogen atoms (Ag−N distances: 2.27 Å and Å 2.32 Å) from two ligands $\mathbf{L^2}$ and three oxygen atoms (Ag−O distance: 2.23−2.84 Å) from one DMF molecule and two weakly coordinated nitrate anions (Figure S8a). The two Ag−N bonds and one Ag−O bond (from DMF) form a distorted trigonal plane with a N−Ag−N angle of 129.8°, and two N−Ag−O angles of 97.5° and 132.8°, respectively. The other two oxygen atoms from two weakly coordinated nitrate anions occupy the two apical positions of the trigonal plane with an O−Ag−O angle of 167.2° (Figure S8a). The Ag^+ ions in the polymeric chain are separated by 13.65 Å with an Ag−Ag−Ag angle of 180.0°. In the solid state, the polymeric complex **3** packs in a layered fashion. Two face-to-face oriented antiparallel polymers **3** stack together via π−π stacking interactions and are embedded to the "grooves" of two other face-orthogonally oriented antiparallel polymeric chains via C−H···π interactions (Figures 4 and S8).

Copper-Mediated Self-Assembly of L and the Structures of the Resulting Supramolecular Complexes (4−7). Reaction of **L** with copper salts [$Cu(NO_3)_2$ and $CuCl_2$] was investigated in two different solvent systems: (1) benzene and acetonitrile, (2) THF. Single crystals of the copper complexes (**4**−**7**) suitable for X-ray analysis were obtained by slow evaporation of their corresponding sample solutions (Supporting Information). The presence of the paramagnetic Cu^{2+} ion rendered the use of NMR spectroscopy impractical to study the solution behaviors of copper(II) complexes. ESI-MS results show peaks at *m*/*z* 709.37, 750.39, and 766.39 for complexes (**4**, **5**, **6**) obtained in the reaction of **L** and $Cu(NO_3)_2$, peaks at 709.37, 750.39 are assigned to [$HCu(\mathbf{L})(ACN).(NO_3)_2$]$^+$ and [$HCu(\mathbf{L})(ACN)_2.(NO_3)_2$]$^+$, respectively, while the peak at 766.39 remains to be correctly assigned to its corresponding copper complex (Figure S9). No assignable peaks were obtained for complex **7** resulting from the reaction of **L** and $CuCl_2$. The ESI-MS results suggest that simple copper complex species exist in the reaction mixtures of **L** and [$Cu(NO_3)_2$, and the copper complexes **5**, **6**, and **7** were formed via polymerization of those simple copper complex species in the crystallization process.

L reacted with $Cu(NO_3)_2$ in benzene and acetonitrile to afford two kinds of crystals **4** (green, major) and **5** (yellow, minor). Single crystal X-ray diffraction analysis established that complex **4** is a 2D coordination polymeric network with the ligand $\mathbf{L^3}$ and Cu^{2+} ion in a 1:1 stoichiometry. The planar network **4** is formed by connecting $\mathbf{L^3}$ and Cu^{2+} via Cu−N bonds and topologically composed of [$\mathbf{Cu_2(L^3)_2}$] rhomboidal and [$\mathbf{Cu_4(L^3)_4}$] hexagonal cage units, as shown in Figure 5. There are two crystallographically nonequivalent copper centers (**Cu1** and **Cu2**) present in **4** (Figure S10a,b). **Cu1** adopts a highly distorted octahedral arrangement and is occupied by three nitrogen atoms (Cu−N distances: 2.04−2.12 Å) from three $\mathbf{L^3}$, and three oxygen atoms (Cu−O distances: 2.09−2.33 Å) from two nitrate counteranions. The three Cu−O bonds and one Cu−N bond form a highly distorted tetragonal plane with the two O−Cu−O angles of 52.4°, 117.1°, and the two O−Cu−N angles of 94.0°, 96.7°, respectively. The two apical positions of the tetragonal plane are occupied by the other two nitrogen atoms with an N−Cu−N angle of 177.2° (Figure S10a). **Cu2** also adopts a highly distorted octahedral arrangement and is occupied by four nitrogen atoms (Cu−N distances: 1.99−2.31 Å) from three $\mathbf{L^3}$ and a coordinated acetonitrile (ACN), and two oxygen atoms (Cu−O distances: 1.98 and 2.52 Å) from one nitrate counteranions. The highly distorted tetragonal plane formed by two Cu−N bonds (one from $\mathbf{L^3}$ and the other from ACN) and the two Cu−O bonds has an O−Cu−O angle of 56.1°, two O−Cu−N angles of 86.2°, 107.2°, and a N−Cu−N angle of 110.5°, respectively. The remaining two nitrogen atoms occupy the two apical positions of the tetragonal plane with a N−Cu−N angle of 176.6° (Figure S10b). In complex **4**, the [$\mathbf{Cu_2(L^3)_2}$] rhomboidal cage is formed by bridging two ligands $\mathbf{L^3}$ by two Cu^{2+} centers (**Cu1** and **Cu2**) with the **Cu1···Cu2** separation of 12.04 Å. A guest nitrate anion is included in this cage via C−H···π (anion) interactions (Figure 5a). The distorted [$\mathbf{Cu_4(L^3)_4}$] hexagonal cage is formed by the connection of four ligands $\mathbf{L^3}$ and four Cu^{2+} cations (two **Cu1** and two **Cu2**). The two Cu^{2+} centers (**Cu1** and **Cu2**) together with the four centers of $\mathbf{L^3}$ are positioned in the six corners of the hexagonal cage. Four pyrazinyl ring planes (**Pyz**) from the four $\mathbf{L^3}$ and the two pyrazinyl-Cu- pyrazinyl (**Pyz-Cu1-Pyz** and **Pyz-Cu2-Pyz**) planes form the six concave surfaces of the hexagonal cage. The **Cu1** and **Cu2** centers positioned in the two opposite corners of the [$\mathbf{Cu_4(L^3)_4}$] hexagonal cage are separated by 24.23 Å, while the **Cu1** and **Cu2** centers positioned in the two **Pyz-Cu-Pyz** planes of the [$\mathbf{Cu_4(L^3)_4}$] hexagonal cage are separated by 10.83 Å. Four disordered benzene molecules are included in the [$\mathbf{Cu_4(L^3)_4}$] hexagonal cage (Figure 5b). The connection of the [$\mathbf{Cu_2(L^3)_2}$] rhomboidal and the [$\mathbf{Cu_4(L^3)_4}$] hexagonal cage motifs resulted in the formation of the planar 2D network complex **4** (Figure 5c). In the solid state, the planar 2D network complexe **4** packs in a staggered manner with an ABAB... sequence with the openings of the metallomacrocyclic cage motifs in each layer being blocked by its neighboring layers sitting from above and below. Thus, no infinite channels are formed (Figure S10c).

X-ray diffraction study revealed that complex **5** (yellow) possesses an infinite 1D coordinative polymeric structure formed by bridging ligands $\mathbf{L^2}$ and Cu^{2+} cations in a 1:1 stoichiometry, which is completely different from that of **4**. The Cu^{2+} centers, as well as ligands $\mathbf{L^2}$, are all crystallographically equivalent in **5**. The Cu^{2+} center adopts a highly distorted trigonal bipyramidal arrangement and is occupied by two nitrogen atoms (Cu−N distances: 2.03 Å, 2.17 Å) from two ligands $\mathbf{L^2}$ and three oxygen atoms (Cu−O distances: 1.91−2.05 Å) from two coordinated nitrate counteranions. The two Cu−N bonds and one Cu−O bond form a distorted trigonal plane with a N−Cu−N angle of 102.0°, and two N−Cu−O angles of 114.4° and 138.2°, respectively. The two apical positions of the trigonal bipyramidal are occupied by the other two coordinated nitrate oxygen atoms with an O−Cu−O angle of 163.3° (Figure S11). The Cu^{2+} cations in the polymeric chain are separated by 12.56 Å with a Cu−Cu−Cu angle of

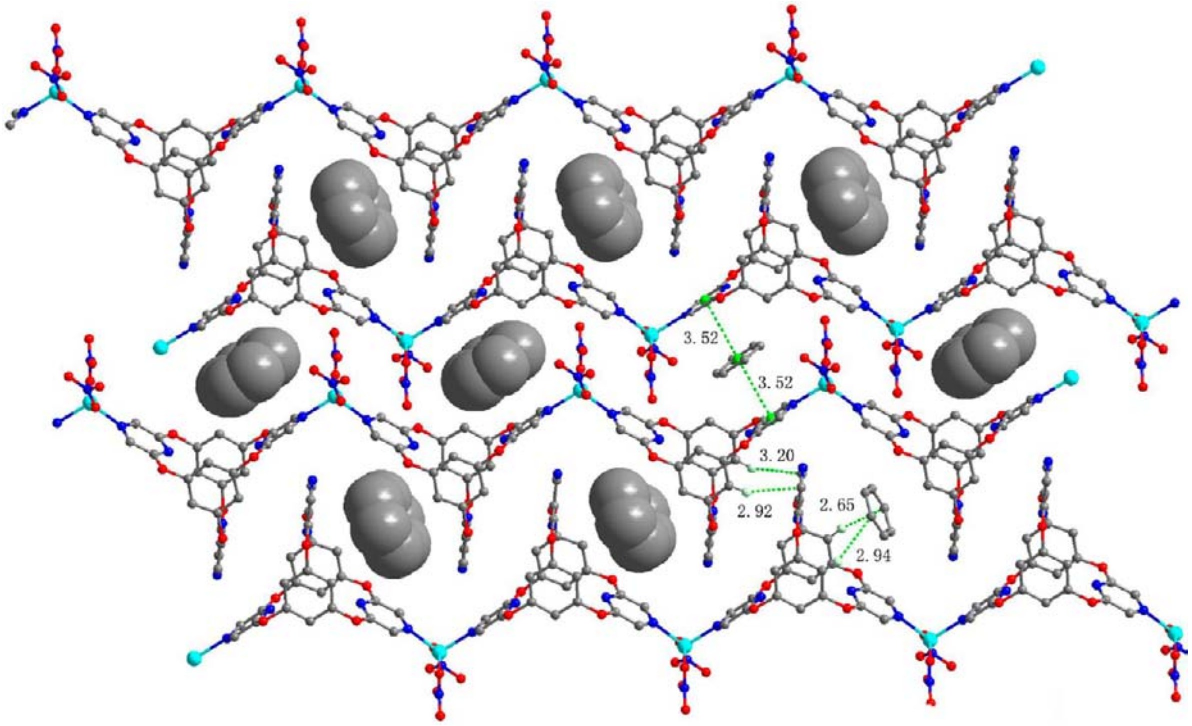

Figure 6. The antiparallel arrangement of the polymeric chains of complexes **5** and their interactions with guest molecules of benzene in the solid state. Hydrogen atoms other than those involved in hydrogen-bonding are omitted for clarity. Color code: Cu (green), O (red), N (blue), C (gray), H (white).

180.0°. The uncoordinated pyrazine planes in $\mathbf{L}^2$ are parallelly arranged along the polymeric chain. In the solid state, complex **5** packs in a layered fashion, and each single chain of **5** in the layer is surrounded by two other antiparallelly arranged chains of **5**. Intermolecular C−H···π interactions between the antiparallelly arranged polymeric chains exists. The voids created by this arrangement act as molecular hosts to encapsulate benzene guests, which are stabilized by C−H···π, as well as π···π stacking interactions, as shown in Figure 6.

L reacted with $Cu(NO_3)_2$ in THF to afford complex **6**. Single crystal X-ray structure analysis established complex **6** as a 2D polymeric network with ligand $\mathbf{L}^3$ and Cu^{2+} ion in a ratio of 1:1. The polymeric network **6** is composed of distorted rectangular cages $[\mathbf{Cu_3(L^3)_3}]$ formed by bridging the tridentate ligands $\mathbf{L}^3$ by Cu^{2+} cations, as shown in Figure 7. In complex **6**, the ligand $\mathbf{L}^3$ and the Cu^{2+} centers are all crystallographically equivalent. $\mathbf{L}^3$ adopts a distorted T-shaped conformation. The Cu^{2+} center adopts a slightly distorted tetragonal pyramidal arrangement and is occupied by three nitrogen atoms (Cu−N distances: 2.09−2.22 Å) from three $\mathbf{L}^3$ and two oxygen atoms (Cu−O distance, 1.97 Å) from two coordinated nitrate counteranions. The two Cu−O bonds and two Cu−N bonds form a distorted tetragonal plane with a N−Cu−N angle of 170.6°, an O−Cu−O angle of 178.3°, and two sets of N−Cu−O angles of 89.3° and 90.6°, respectively. The other coordinated nitrogen atom thus occupies the apical position of the tetragonal plane (Figure S12a). In the distorted $[\mathbf{Cu_3(L^3)_3}]$ rectangular cage, two Cu^{2+} cations and two centers of $\mathbf{L}^3$ are positioned in the four corners of the cage, while the other Cu^{2+} cation is positioned in the middle of one **Pyz-Cu-Pyz** edge (Figure 7). The three Cu^{2+} cations in the $[\mathbf{Cu_3(L^3)_3}]$ rectangular cage are separated by 11.48 Å, 12.23 Å, and 14.49 Å, respectively. Each Cu^{2+} cation, as well as each $\mathbf{L}^3$ in **6**, is involved in the formation of three $[\mathbf{Cu_3(L^3)_3}]$ rectangular cages and plays the roles as edge or corners in these three rectangular cages. The void of the $[\mathbf{Cu_3(L^3)_3}]$ rectangular cage acts as a molecular host to encapsulate two THF guest molecules (Figure 7). In the solid state, layers of complex **6** pack in staggered fashion with an ABAB... sequence viewed along the *b*-axis, and thus no $[\mathbf{Cu_3(L^3)_3}]$ rectangular channels are formed in the solid state (Figure S12).

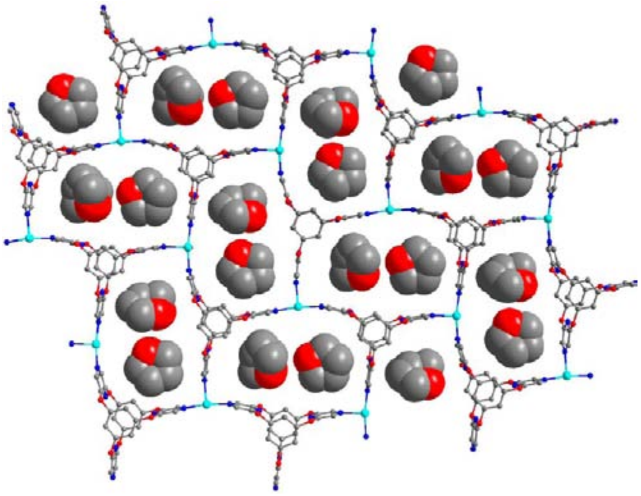

Figure 7. The 2D polymeric network structure of complex **6** comprised of distorted rectangular cage motif $[\mathbf{Cu_3(L^3)_3{\cdot}2THF}]$ in which two guest molecules of THF are included. Nitrate anions and hydrogen atoms are omitted for clarity. Color code: Cu (green), O (red), N (blue), C (gray).

L reacted with $CuCl_2$ in THF to afford complex **7**. Single crystal X-ray analysis revealed that complex **7** possesses an

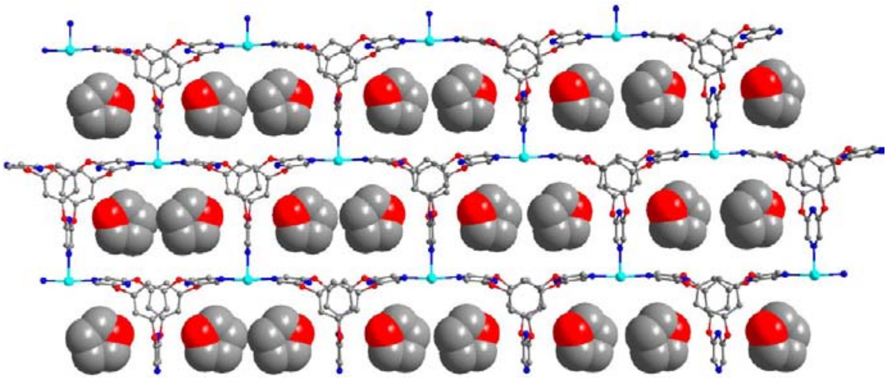

Figure 8. The 2D polymeric network structure of complex **7** with a "brick wall"-like topology comprised of highly symmetrical rectangular cage motif $[\mathbf{Cu_3(L^3)_3{\cdot}2THF}]$ in which two guest molecules of THF are included. Chlorides and hydrogen atoms are omitted for clarity. Color code: Cu (green), O (red), N (blue), C (gray), Cl (yellow).

infinite 2D polymeric network structure comprising highly symmetrical $[\mathbf{Cu_3(L^3)_3}]$ rectangular cage motifs which are formed by connection of three ligands $\mathbf{L^3}$ and three Cu^{2+} cations, as shown in Figure 8. In complex **7**, the ligand $\mathbf{L^3}$ and the Cu^{2+} centers are crystallographically equivalent, and ligand $\mathbf{L^3}$ adopts a T-shaped conformation, similar to that in **6**. The Cu^{2+} center adopts a distorted trigonal bipyramidal arrangement and is occupied by three nitrogen atoms (Cu−N distances: 2.14−2.18 Å) from three ligands $\mathbf{L^3}$ and two chloride atoms (Cu−Cl distance: 2.27 Å). Each Cu^{2+} center, as well as each $\mathbf{L^3}$ in **7**, is involved in the formation of three identical $[\mathbf{Cu_3(L^3)_3}]$ rectangular cages. The two Cu−Cl bonds and one Cu−N bond form a distorted trigonal plane with a Cl−Cu−Cl angle of 141.5° and two Cl−Cu−N angles of 109.3°, respectively. The other two coordinated nitrogen atoms occupy the two apical positions of the trigonal bipyramidal with a N_{ap}−Cu−N_{ap} angle of 175.9° (Figure S13). In the highly symmetrical $[\mathbf{Cu_3(L^3)_3}]$ rectangular cage, two Cu^{2+} cations and two $\mathbf{L^3}$ centers occupy the four corners of the cage, and the remaining Cu^{2+} cation is placed in the middle of one edge (**Pyz-Cu-Pyz**), similar to that in complex **6**. The three Cu^{2+} cations in the $[\mathbf{Cu_3(L^3)_3}]$ cage form an isosceles triangle with the Cu···Cu separations of 11.72 Å, 11.72 Å, and 14.46 Å, respectively. The $[\mathbf{Cu_3(L^3)_3}]$ rectangular cages in complex **7** are topologically "brick-shaped", and thus, the overall structure of complex **7** possesses a "brick wall"-like topology. Each $[\mathbf{Cu_3(L^3)_3}]$ rectangular cage acts as a molecular host to host two THF molecules (Figure 8). In the solid state, complex **7** packs in staggered layers in an ABAB... sequence with layers A and B oriented in opposite directions viewed along the *c*-axis (Figure S13).

Zinc-Mediated Self-Assembly of L and the Structures of the Resulting Supramolecular Complexes (8−11). Reaction of **L** with Zn^{2+} cations $[Zn(NO_3)_2$ and $ZnI_2]$ were also investigated in two solvent systems: (1) benzene and acetonitrile, (2) THF. Single crystals of the corresponding zinc complexes (**8**−**11**) suitable for X-ray analysis were obtained by slow evaporation of their sample solutions (Supporting Information). ^{1}H NMR spectra of Zn^{2+} complexes (**8** and **9**) in solvents, such as DMSO-d_6, CD_3CN, DMF-d_7, and CD_3OD, showed no proton shifts compared to the corresponding free ligand **L**, suggesting that the Zn^{2+} complexes do not survive in these coordinating solvents. The ^{1}H NMR spectrum of **8** in CD_3NO_2, however, shows a downfield shift (0.42 ppm) of the pyrazinyl proton signals (compared to that of the free ligand), indicating some complex species $[Zn_n\mathbf{L}_m]^{2n+}$ exist in CD_3NO_2, and these species are under fast equilibration on the NMR time scale (Figure S14). No shifts were observed in the ^{1}H NMR spectrum of **9** in CD_3NO_2, possibly due to the existence of coordinative THF molecules in the system. ESI-MS result shows peaks at *m*/*z* 663.45 and 859.51 for **8** and **9** in acetonitrile solution, and these peaks remain to be correctly assigned to their corresponding zinc complex species. Because of the extremely low solubility of the zinc complexes **10** and **11** formed by **L** and ZnI_2, it is technically difficult to investigate their solution properties by NMR and ESI-MS techniques.

L reacted with $Zn(NO_3)_2$ in benzene and acetonitrile to afford colorless crystals of **8**. Single crystal X-ray analysis revealed that the structure of complex **8** is essentially identical, as crystallographically isostructural and isomorphous, to the structure of **5** (Figure S15). All of the comments applied to the Cu-based coordination polymer **5** are equally applied to the Zn-based coordination polymer **8**. Slight differences in metal−ligand bond distances are observed between complexes **5** and **8** (Zn−N distances in **8**, 2.03 Å and 2.06 Å; Zn−O distances in **8**, 1.98−2.37 Å). The Zn^{2+} cations are separated by 12.60 Å in the polymeric chain of **8**.

L reacted with $Zn(NO_3)_2$ in THF to afford colorless crystals of **9**. Single crystal X-ray analysis revealed that the structure of complex **9** is crystallographically isomorphous, to the structure of **7**. The structural difference between **7** and **9** lies on coordination geometries adopted by Cu^{2+} in **7** and Zn^{2+} in **9**, coordinated counteranions for Cu^{2+} in **7** (Cl^-) and Zn^{2+} in **9** (NO_3^-), and the corresponding bond lengths and angles (Figure S16). In complex **9**, the Zn^{2+} center adopts a distorted pentagonal bipyramidal arrangement and is occupied by three nitrogen atoms (Zn−N distances, 2.09 Å and 2.22 Å) from three ligands $\mathbf{L^3}$ and four oxygen atoms (Zn−O distances, 2.18 Å and 2.34 Å) from two bis-coordinated nitrate anions. The four Zn−O bonds and one Zn−N bond form a highly distorted pentagonal plane, and the two apical positions of the pentagonal bipyramidal are occupied by two pyrazinyl nitrogen atoms with an N−Zn−N angle of 179.5°. Similarly, each $[\mathbf{Zn_3(L^3)_3}]$ rectangular cage in **9** hosts two THF molecules in the solid state.

L reacted with ZnI_2 in benzene and acetonitrile to afford colorless crystals of **10**. The crystallographically isomorphous nature of complex **10** with complexes **5** and **8** is established by single crystal X-ray analysis (Figure S17). In complex **10**, the Zn^{2+} center adopts a distorted tetrahedral arrangement and is occupied by two nitrogen atoms (Zn−N distances, 2.09 Å and 2.10 Å) from two ligands $\mathbf{L}^2$ and two iodine atoms (Zn−I distances, 2.53 Å and 2.55 Å), with the N−Zn−N angle of 104.9°, I−Zn−I angle of 121.8°, and the two N−Zn−I angles of 106.6° and 108.3°, respectively. The Zn^{2+} cations are separated by 12.77 Å in the polymeric chain **10** with the Zn−Zn−Zn angles of 180.0°. In the solid state, complex **10** packs similarly to those of complexes **5** and **8**, and guest molecules of benzene are hosted in the crystal lattice via C−H···π and π···π stacking interactions. Intermolecular hydrogen−iodine bonds between the pyrazinyl protons and iodine atoms in the neighboring layers are also observed (CH···I, 3.18 Å, C−H−I, 138.1°).

L reacted with ZnI_2 in THF to afford colorless crystals of **11**. Complex **11** was crystallographically established as isostructural and isomorphous, to the structure of **7**. All of the comments applied to the Cu-based coordination polymer **7** are equally applied to the Zn-based coordination polymer **11**. Because of the vibrational nature of the Zn^{2+} cations, the exact Zn−N and Zn−I bond lengths, as well as the Zn^{2+} centered angles, could not been fully refined. Similar to complex **7**, the $[\mathbf{Zn_3(L^3)_3}]$ rectangular cage unit in **11** hosts two THF molecules in the solid state (Figure S18).

■ CONCLUSION

A novel tris-pyrazinyl-pillared prismatic bicycooxacalixaromatic ligand **L** was successfully synthesized and structurally characterized. The coordination-driven self-assembly of **L** with three metal cations (Ag^+, Cu^{2+}, Zn^{2+}) afforded a diverse set of 1D and 2D coordination polymers **1**−**11**, in which **L** acts as both bidentate ($\mathbf{L}^2$) and tridentate ($\mathbf{L}^3$) connecting nodes. The core metal ions (Ag^+, Cu^{2+}, Zn^{2+}), counteranions, as well as the solvent systems employed in the self-assembly processes, all have significant impacts on the topologies of the resultant self-assembled metallosupramolecular polymers. The metallo-rectangular, rhomboidal, and hexagonal cage motifs with "thicker walls", present in the coordination self-assembled polymeric structures, can act as molecular hosts to encapsulate a range of neutral and charged guest species. The results demonstrate the advantage of the preorganized 3D cagelike ligands in the construction of unconventional supramolecular architectures with unprecedented metallomacrocyclic cage motifs. Further research work will be focused on the application of such ligands in the construction of sophisticated polymeric metallosupramolecular networks with advanced functionalities.

■ ASSOCIATED CONTENT

Ⓢ Supporting Information

^{1}H and ^{13}C NMR spectra for ligand **L**, ^{1}H NMR spectra, ESI-MS results, molecular structures, molecular packings of some reported metal complexes of **L**, CIF files of **1** and all reported metal complexes. This material is available free of charge via the Internet at http://pubs.acs.org.

■ AUTHOR INFORMATION

Corresponding Author

*Tel: +86-21-20325166-8003; fax: +86-21-20325173; e-mail: wenk@sari.ac.cn, kwen@brain.ecnu.edu.cn(K.W.); jiangb@sari.ac.cn (B.J.), mlma@brain.ecnu.edu.cn (M.-L.M.).

Notes

The authors declare no competing financial interest.

■ ACKNOWLEDGMENTS

The authors thank the National Natural Science Foundation of China (21071053, 21002031, 61078071), Shanghai Commission for Science and Technology (06Pj14034, 10ZR1409700, 09ZR1422500); support by the "Strategic Priority Research Program" of the Chinese Academy of Sciences (XDA01020304) is acknowledged.

■ REFERENCES

(1) For reviews, see: (a) Leininger, S.; Olenyuk, B.; Stang, P. J. *Chem. Rev.* **2000**, *100*, 853. (b) Seidel, S. R.; Stang, P. J. *Acc. Chem. Res.* **2002**, *35*, 792. (c) Kawano, M.; Fujita, M. *Coord. Chem. Rev.* **2007**, *251*, 2592. (d) Lee, S. J.; Lin, W. B. *Acc. Chem. Res.* **2008**, *41*, 521. (e) Dalgarno, S. J.; Power, N. P.; Atwood, J. L. *Coord. Chem. Rev.* **2008**, *252*, 825. (f) Northorp, B. H.; Zheng, Y.-R.; Chi, K.-W.; Stang, P. J. *Acc. Chem. Res.* **2009**, *42*, 1554. (g) Ward, M. D. *Chem. Commun.* **2009**, 4487. (h) Leong, W. L.; Vitta, J. J. *Chem. Rev.* **2011**, *111*, 688. (i) Chakrabarty, R.; Mukherjee, P. S.; Stang, P. J. *Chem. Rev.* **2011**, *111*, 6810.

(2) (a) Kesanli, B.; Lin, W. B. *Coord. Chem. Rev.* **2003**, *246*, 305. (b) Fiedler, D.; Leung, D. H.; Bergman, R. G.; Raymond, K. N. *Acc. Chem. Res.* **2005**, *38*, 349. (c) Li, J.-R.; Kuppler, R. J.; Zhou, H.-C. *Chem. Soc. Rev.* **2009**, *38*, 1477. (d) Li, J.-R.; Sculley, J.; Zhou, H.-C. *Chem. Rev.* **2012**, *112*, 869. (e) Huang, L. M.; Wang, H. T.; Chen, J. X.; Wang, Z. B.; Sun, J. Y.; Zhao, D. Y.; Yan, Y. S. *Microporous Mesoporous Mater.* **2003**, *58*, 105. (f) Leung, D. H.; Bergman, R. G.; Raymond, K. N. *J. Am. Chem. Soc.* **2006**, *128*, 9781. (g) Li, G.; Yu, W.; Cui, Y. *J. Am. Chem. Soc.* **2008**, *130*, 4582. (h) Zhang, J.-P.; Chen, X.-M. *J. Am. Chem. Soc.* **2008**, *130*, 6010. (i) Alaerts, L.; Maes, M.; Giebeler, L.; Jacobs, P. A.; Martens, J. A.; Denayer, J. F. M.; Kirschhock, C. E. A.; De Vos, D. E. *J. Am. Chem. Soc.* **2008**, *130*, 14170.

(3) (a) Lee, J.; Farha, O. K.; Roberts, J.; Scheidt, K. A.; Nguyen, S. T.; Hupp, J. T. *Chem. Soc. Rev.* **2009**, *38*, 1450. (b) Yoon, M.; Srirambalaji, R.; Kim, K. *Chem. Rev.* **2012**, *112*, 1196. (c) Fujita, M.; Kwon, Y. J.; Washizu, Ogura, S. K. *J. Am. Chem. Soc.* **1994**, *116*, 1151. (d) Seo, J. S.; Whang, D.; Lee, H.; Jun, S. I.; Oh, J.; Jeon, Y. J.; Kim, K. *Nature* **2000**, *404*, 982. (e) Merlau, M. L.; Del Pilar Mejia, M.; Nguyen, S. T.; Hupp, J. T. *Angew. Chem., Int. Ed.* **2001**, *40*, 4239. (f) Hu, A. G.; Ngo, H. L.; Lin, W. B. *J. Am. Chem. Soc.* **2003**, *125*, 11490. (g) Wu, C.; Hu, A.; Zhang, L.; Lin, W. B. *J. Am. Chem. Soc.* **2005**, *127*, 8940. (h) Uemura, T.; Kitaura, R.; Ohta, Y.; Nagaoka, M.; Kitagawa, S. *Angew. Chem., Int. Ed.* **2006**, *45*, 4112. (i) Yoshizawa, M.; Tamura, M.; Fujita, M. *Science* **2006**, *312*, 251. (j) Pluth, M. D.; Bergman, R. G.; Raymond, K. N. *Science* **2007**, *316*, 85. (k) Yoon, H. J.; Kuwabara, J.; Kim, J.-H.; Mirkin, C. A. *Science* **2010**, *330*, 66. (l) Hastings, C. J.; Pluth, M. D.; Bergman, R. G.; Raymond, K. N. *J. Am. Chem. Soc.* **2010**, *132*, 6938. (m) Murase, T.; Nishijima, Y.; Fujita, M. *J. Am. Chem. Soc.* **2012**, *134*, 162.

(4) (a) Eddaoudi, M.; Moler, D. B.; Li, H.; Chen, B.; Reineke, T. M.; O'Keeffe, M. O.; Yaghi, O. M. *Acc. Chem. Res.* **2001**, *34*, 319. (b) Moulton, B.; Zaworotko, M. J. *Chem. Rev.* **2001**, *101*, 1629. (c) Fèrey, G. *Chem. Soc. Rev.* **2008**, *37*, 191. (d) Getman, R. B.; Bae, Y.-S.; Wilmer, C. E.; Snurr, R. Q. *Chem. Rev.* **2012**, *112*, 703. (e) Sumida, K.; Rogow, D. L.; Mason, J. A.; McDonald, T. M.; Bloch, E. D.; Z. Herm, R.; Bae, T.-H.; Long, J. R. *Chem. Rev.* **2012**, *112*, 724. (f) Suh, M. P.; Park, H. J.; Prasad, T. K.; Lim, D.-W. *Chem. Rev.* **2012**, *112*, 782. (g) Batten, S. R.; Robson, R. *Angew. Chem., Int. Ed.* **1998**, *37*, 1460. (h) Wong-Foy, A. G.; Matzger, A. J.; Yaghi, O. M. *J. Am. Chem. Soc.* **2006**, *128*, 3494. (i) Ma, S.; Sun, D.; Simmons, J. M.; Collier, C. D.; Yuan, D.; Zhou, H.-C. *J. Am. Chem. Soc.* **2008**, *130*, 1012. (j) Caskey, S. R.; Wong-Foy, A. G.; Matzger, A. J. *J. Am. Chem. Soc.* **2008**, *130*, 10870. (k) Britt, D.; Tranchemontagne, D.; Yaghi, O. M. *Proc. Natl. Acad. Sci. U. S. A.* **2008**, *105*, 11623. (l) Zhang, J.-P.; Chen, X.-M. *J. Am. Chem. Soc.* **2009**, *131*, 5516.

(5) (a) Yoshizawa, M.; Klosterman, J. K.; Fujita, M. *Angew. Chem., Int. Ed.* **2009**, *48*, 3418. (b) Yoshizawa, M.; Kusukawa, T.; Fujita, M.; Sakamoto, S.; Yamagushi, K. *J. Am. Chem. Soc.* **2001**, *123*, 10454. (c) Yoshizawa, M.; Tamura, M.; Fujita, M. *Science* **2006**, *312*, 251.

(d) Dong, V. M.; Fiedler, D.; Carl, B.; Bergman, R. G.; Raymond, K. N. *J. Am. Chem. Soc.* **2006**, *128*, 14464. (e) Kuil, M.; Soltner, T.; van Leeuwen, P. W. N. M.; Reek, J. N. H. *J. Am. Chem. Soc.* **2006**, *128*, 11344. (f) Lee, S. J.; Cho, S.-H.; Mulfort, K. L.; Tiede, D. M.; Hupp, J. T.; Nguyen, S. T. *J. Am. Chem. Soc.* **2008**, *130*, 16828. (g) Mal, P.; Breiner, B.; Rissanen, K.; Nitschke, J. R. *Science* **2009**, *324*, 1697. (h) Ohara, K.; Inokuma, Y.; Fujita, M. *Angew. Chem., Int. Ed.* **2010**, *49*, 5507. (I) Ikemoto, K.; Inokuma, Y.; Fujita, M. *Angew. Chem., Int. Ed.* **2010**, *49*, 5750. (j) Sarmentero, M. A.; Fernandez, P. H.; Zuidema, E.; Bo, C.; Vidal, F. A.; Ballester, P. *Angew. Chem., Int. Ed.* **2010**, *49*, 7489. (k) Smulders, M. M. J.; Nitschke, J. R. *Chem. Sci.* **2012**, *3*, 785. (l) Inokuma, Y.; Ning, G.-N.; Fujita, M. *Angew. Chem., Int. Ed.* **2012**, *51*, 2379.

(6) For reviews, see: (a) Steel, P. J. *Acc. Chem. Res.* **2005**, *38*, 243. (b) Hosseini, M. W. *Acc. Chem. Res.* **2005**, *38*, 313. (c) Fujita, M.; Tominaga, M.; Hori, A.; Therrien, B. *Acc. Chem. Res.* **2005**, *38*, 371. (d) Zhao, D.; Timmons, D. J.; Yuan, D.; Zhou, H.-C. *Acc. Chem. Res.* **2011**, *44*, 123. (e) Almeida Paz, F. A.; Klinowski, J.; Vilela, S. M. F.; Tomè, J. P. C.; Cavaleiro, J. A. S.; Rocha, J. *Chem. Soc. Rev.* **2012**, *41*, 1088.

(7) (a) Cahn, R. S.; Ingold, C.; Prelog, V. *Angew. Chem., Int. Ed. Engl.* **1966**, *5*, 385. (b) Lehn, J.-M.; Sauvage, J.-P.; Simon, J.; Ziesel, R. *New J. Chem.* **1983**, *7*, 413. (c) Dietrich-Bechecker, C. O.; Sauvage, J.-P. *Angew. Chem., Int. Ed. Engl.* **1989**, *28*, 189. (d) Funeriu, D. P.; Lehn, J. M.; Baum, G.; Denske, D. *Chem.—Eur. J.* **1997**, *7*, 99. (e) Cui, Y.; Lee, S. J.; Lin. *J. Am. Chem. Soc.* **2003**, *125*, 6014. (f) Chichak, K. S.; Cantrill, S. J.; Pease, A. R.; Chiu, S.-H.; Cave, G. W. V.; Atwood, J. L.; Stoddart, J. F. *Science* **2004**, *304*, 1308. (g) W. Zhang, S.; Yang, S.; Lan, J.; Yang, S.; You, J. *Chem. Coummun.* **2008**, 6710. (h) Uemura, K.; Kumamoto, Y.; Kitagawa, S. *Chem.—Eur. J.* **2008**, *14*, 9565. (i) Weilandt, T.; Kiehne, U.; Bunzen, J.; Schnakenburg, G.; Lützen, A. *Chem.—Eur. J.* **2010**, *26*, 2418. (j) Arouss, B. E.; Zebret, S.; Besnard, C.; Perrottet, P.; Hamacek, J. *J. Am. Chem. Soc.* **2011**, *133*, 10764.

(8) (a) Yang, H. B.; Ghosh, K.; Northrop, B. H.; Stang, P. J. *Org. Lett.* **2007**, *9*, 1561. (b) Yang, H.-B.; Hawkridge, A. M.; Huang, S. D.; Das, N.; Bunge, S. D.; Muddiman, D. C.; Stang, P. J. J. *J. Am. Chem. Soc.* **2007**, *129*, 2120. (c) Yang, H.-B.; Ghosh, K.; Northrop, B. H.; Zheng, Y.-R.; Lyndon, M. M.; Muddiman, D. C.; Stang, P. J. J. *J. Am. Chem. Soc.* **2007**, *129*, 14187. (d) Caskey, D. C.; Yamamoto, T.; Addicott, C.; Shoemaker, R. K.; Vacek, J.; Hawkridge, A. M.; Muddiman, D. C.; Kottas, G. S.; Michl, J.; Stang, P. J. *J. Am. Chem. Soc.* **2008**, *130*, 7620. (e) Zheng, Y.-R.; Zhao, Z.; Wang, M.; Ghosh, K.; Pollock, J. B.; Cook, T. R.; Stang, P. J. J. *J. Am. Chem. Soc.* **2010**, *132*, 16873. (f) Han, Q.; Li, Q.-J.; He, M.; Hu, B.; Tan, H.; Abliz, Z.; Wang, C.-H.; Yu, Y.; Yang, H.-B. *J. Org. Chem.* **2011**, *76*, 9660.

(9) (a) Fujita, M.; Nagao, S.; Ogura, K. *J. Am. Chem. Soc.* **1995**, *117*, 1649. (b) Kumazawa, K.; Yamanoi, Y.; Yoshizawa, M.; Kusukawa, T.; Fujita, M. *Angew. Chem., Int. Ed.* **2004**, *43*, 5936. (c) Tashiro, S.; Kobayashi, M.; Fujita, M. *J. Am. Chem. Soc.* **2006**, *128*, 9280. (d) Tidmarsh, I. S.; Faust, T. B.; Adams, H.; Harding, L. P.; Russo, L.; Clegg, W.; Ward, M. D. *J. Am. Chem. Soc.* **2008**, *130*, 15167. (e) Sawada, T.; Yoshizawa, M.; Sato, S.; Fujita, M. *Nat. Chem.* **2009**, *1*, 53. (f) Clever, G. H.; Tashiro, M.; Shionoya, M. *Angew. Chem., Int. Ed.* **2009**, *48*, 7010. (g) Hatakeyama, Y.; Sawada, T.; Kawano, M.; Fujita, M. *Angew. Chem., Int. Ed.* **2009**, *48*, 8695. (h) Yamauchi, Y.; Yoshizawa, M.; Akita, M.; Fujita, M. *Proc. Natl. Acad. Sci. U. S. A.* **2009**, *106*, 10435. (i) Sun, Q.-F.; Iwasa, J.; Ogawa, D.; Ishido, Y.; Sato, S.; Ozeki, T.; Sei, Y.; Yamaguchi, K.; Fujita, M. *Science* **2010**, *328*, 1144. (j) Kishi, N.; Li, Z.; Yoza, K.; Akita, M.; Yoshizawa, M. *J. Am. Chem. Soc.* **2011**, *133*, 11438. (k) Sun, Q.-F.; Murase, T.; Sato, S.; Fujita, M. *Angew. Chem., Int. Ed.* **2011**, *50*, 10318. (l) Schmitt, F.; Freudenreich, J.; Barry, N. P. E.; Juillerat-Jeanneret, L.; Süss-Fink, G.; Therrien, B. *J. Am. Chem. Soc.* **2012**, *134*, 754. (m) Freye, S.; Hey, J.; Torras-Galán, A.; Stalke, D.; Herbst-Irmer, R.; John, M.; Clever, G. H. *Angew. Chem., Int. Ed.* **2012**, *51*, 2191. Custelcean, R.; Bonnesen, P. V.; Duncan, N. C.; Zhang, X.; Watson, L. A.; Van Berkel, G.; Parson, W. B.; Hay, B. P. *J. Am. Chem. Soc.* **2012**, *134*, 5825.

(10) (a) Papaefstathiou, G. S.; MacGillivray, L. R. *Angew. Chem., Int. Ed.* **2002**, *41*, 2070. (b) Papaefstathiou, G. S.; Friščić, T.; MacGillivray, L. R. *J. Am. Chem. Soc.* **2005**, *127*, 14160. (c) Halper, S. R.; Do, L.; Stork, J. R.; Cohen, S. M. *J. Am. Chem. Soc.* **2006**, *128*, 15255. (d) Bosch, E.; Barnes, C. L.; Brennan, N. L.; Eakins, G. L.; Breyfogle, B. E. *J. Org. Chem.* **2008**, *73*, 3931. (e) Yan, Li.; Xue, Y.; Gao, G.; Lan, J.; Yang, F.; Su, X.; You, J. *Chem.—Eur. J.* **2010**, *16*, 2250. (f) Hamilton, T. D.; Bučar, D.-K.; Baltrusaitis, J.; Flanagan, D. R.; Li, Y.; Ghorai, S.; Tivanski, A. V.; MacGillivray, L. R. *J. Am. Chem. Soc.* **2011**, *133*, 3365. (g) Wang, J.-L.; Li, X.; Lu, X.; Hsieh, I.-F.; Cao, Y.; Moorefield, C. N.; Wesdemiotis, C.; Cheng, S. Z. D.; Newkome, G. R. *J. Am. Chem. Soc.* **2011**, *133*, 11450. (h) Fu, Z.; Zeng, Y.; Liu, X.; Song, D.; Liao, S.; Dai, J. *Chem. Commun.* **2012**, *48*, 6154. (i) Schultz, A.; Li, X.; Barkakaty, B.; Moorefield, C. N.; Wesdemiotis, C.; Newkome, G. R. *J. Am. Chem. Soc.* **2012**, *134*, 7672.

(11) (a) Molenveld, P.; Engbersen, J. F. J.; Reinhoudt, D. N. *Chem. Soc. Rev.* **2000**, *29*, 75. (b) *Calixarenes in Action*; Mandolini, L.; Ungaro, R., Eds.; Imperial College Press: London, 2000.

(12) (a) Rebek, J. *Acc. Chem. Rev.* **1999**, *32*, 278. (b) Warmuth, R.; Yoon, J. *Acc. Chem. Rev.* **2001**, *34*, 95. (c) Nishimura, N.; Kobayashi, K. *Angew. Chem., Int. Ed.* **2008**, *47*, 6255.

(13) (a) Zhong, Z.; Ikeda, A.; Ayabe, M.; Shinkai, S.; Sakamoto, S.; Yamaguchi, K. *J. Org. Chem.* **2001**, *66*, 1002. (b) Cotton, F. A.; Lei, P.; Lin, C.; Murillo, C. A.; Wang, X.; Yu, S.-Y.; Zhang, Z.-X. *J. Am. Chem. Soc.* **2004**, *126*, 1518. (c) Dalgarno, S. J.; Claudio-Bosque, K. M.; Warren, J. E.; Glass, T. E.; Atwood, J. L. *Chem. Commun.* **2008**, 1410.

(14) (a) Jacopozzi, P.; Dacanale, E. *Angew. Chem., Int. Ed.* **1997**, *36*, 613. (b) Fox, O. D.; Dalley, N. K.; Harrison, R. G. *J. Am. Chem. Soc.* **1998**, *120*, 7111. (c) Fox, O. D.; Drew, M. G. B.; Beer, P. D. *Angew. Chem., Int. Ed.* **2000**, *39*, 136. (d) Fox, O. D.; Drew, M. G. B.; Wilkinsona, E. J. S.; Beer, P. D. *Chem. Commun.* **2000**, 391. (e) Fochi, F.; Jacopozzi, P.; Wegelius, E.; Rissanen, K.; Cozzini, P.; Marastoni, E.; Fisicaro, E.; Manini, P.; Fokkens, R.; Dalcanale, E. *J. Am. Chem. Soc.* **2001**, *123*, 7539. (f) Park, S. J.; Hong, J.-I. *Chem. Commun.* **2001**, 1554. (g) Pirondini, L.; Bertolini, F.; Cantadori, B.; Ugozzoli, F.; Massera, C.; Dalcanale, E. *Proc. Natl. Acad. Sci. U. S. A.* **2002**, *99*, 4911. (h) Bibal, B.; Tinant, B.; Declercq, J.-P.; Dutasta, J.-P. *Chem. Commun.* **2002**, 432. (i) Menozzi, E.; Pinalli, R.; Speets, E. A.; Jan Ravoo, B.; Dalcanale, E.; Reinhoudt, D. N. *Chem.—Eur. J.* **2004**, *10*, 2199. (j) Pinalli, R.; Cristini, V.; Sottili, V.; Geremia, S.; Campagnolo, M.; Caneschi, A.; Dalcanale, E. *J. Am. Chem. Soc.* **2004**, *126*, 6516. (k) Kobayashi, K.; Yamada, Y.; Yamanaka, M.; Sei, Y.; Yamaguchi, K. *J. Am. Chem. Soc.* **2004**, *126*, 13896. (l) McKinlay, R. M.; Thallapally, P. K.; Cave, G. W. V.; Atwood, J. L. *Angew. Chem., Int. Ed.* **2005**, *44*, 5733. (m) Haino, T.; Kobayashi, M.; Chikaraishi, M.; Fukazawa, Y. *Chem. Commun.* **2005**, 2321. (n) Power, N. P.; Dalgarno, S. J.; Atwood, J. L. *Angew. Chem., Int. Ed.* **2007**, *46*, 8601. (o) Jin, P.; Dalgarno, S. J.; Barnes, C.; Teat, S. J.; Atwood, J. L. *J. Am. Chem. Soc.* **2008**, *130*, 1726. (p) Schröer, T.; Brodbeck, R.; Letzel, M. C.; Mix, A.; Schnatwinkel, B.; Tonigold, M.; Volkmer, D.; Mattay, J. *Tetrahedron Lett.* **2008**, *49*, 5939. (q) Kumari, H.; Mossine, A. V.; Kline, S. R.; Dennis, C. L.; Fowler, D. A.; Teat, S. J.; Barnes, C. L.; Deakyne, C. A.; Atwood, J. L. *Angew. Chem., Int. Ed.* **2012**, *51*, 1452.

(15) (a) Zhong, Z.; Ikeda, A.; Shinkai, S.; Sakamoto, S.; Yamaguchi, K. *Org. Lett.* **2001**, *3*, 1085. (b) Sumby, C. J.; Hardie, M. J. *Angew. Chem., Int. Ed.* **2005**, *44*, 6395. (c) Sumby, C. J.; Prior, T. J.; Hardie, M. J. *Chem.—Eur. J.* **2006**, *12*, 2945. (d) Sumby, C. J.; Carr, M. J.; Franken, A.; Kennedy, J. D.; Kilner, C. A.; Hardie, M. J. *New J. Chem.* **2006**, *30*, 1390. (e) Ronson, T. K.; Fisher, J.; Harding, L. P.; Hardie, M. J. *Angew. Chem., Int. Ed.* **2007**, *46*, 9086.

(16) (a) Westcott, A.; Fisher, J.; Harding, L. P.; Rizkallah, P. J.; Hardie, M. L. *J. Am. Chem. Soc.* **2008**, *130*, 2950. (b) Little, M. A.; Ronson, T. K.; Hardie, M. J. *Dalton Trans.* **2011**, *40*, 12217.

(17) Ronson, T. K.; Fisher, J.; Harding, L. P.; Rizkallah, P. J.; Warren, J. E.; Hardie, M. L. *Nat. Chem.* **2009**, *1*, 212.

(18) (a) Ma, M.-L.; Wang, H.-X.; Li, X.-Y.; Liu, L.-Q.; Jin, H.-S.; Wen, K. *Tetrahedron* **2009**, *65*, 300. (b) Li, M.; Ma, M.-L.; Li, X.-Y.; Wen, K. *Tetrahedron* **2009**, *65*, 4639. (c) Hu, W.-J.; Zhao, X.-L.; Ma,

M.-L.; Guo, F.; Mi, X.-Q.; Jiang, B.; Wen, K. *Eur. J. Org. Chem.* **2012**, 1448.

(19) (a) Katz, J. L.; Feldman, M. B.; Conry, R. R. *Org. Lett.* **2005**, *7*, 91. (b) Maes, W.; Rossom, W. V.; Van Hecke, K.; Van Meervelt, L.; Dehaen, W. *Org. Lett.* **2006**, *8*, 4161. (c) Wang, L.-X.; Wang, D.-X.; Huang, Z.-T.; Wang, M.-X. *J. Org. Chem.* **2010**, *75*, 741.

(20) For recent reviews, see: (a) König, B.; Fonseca, M. H. *Eur. J. Inorg. Chem.* **2000**, 2303. (b) Maes, W.; Dehaem, W. *Chem. Soc. Rev.* **2008**, *37*, 2393. (c) Wang, M.-X. *Chem. Commun.* **2008**, 4541. (d) Wang, M.-X. *Acc. Chem. Res.* **2012**, *45*, 182.

(21) (a) Ma, M.-L.; Li, X.-Y.; Wen, K. *J. Am. Chem. Soc.* **2009**, *131*, 8338. (b) Li, X.-Y.; Liu, L.-Q.; Ma, M.-L.; Zhao, X.-L.; Wen, K. *Dalton Trans.* **2010**, *39*, 8646. (c) Ma, M.-L.; Li, X.-Y.; Zhao, X.-L.; Guo, F.; Jiang, B.; Wen, K. *CrystEngComm* **2011**, *13*, 1572. (d) Wu, J.-C.; Zhao, L.; Wang, D.-X.; Wang, M.-X. *Inorg. Chem.* **2012**, *51*, 3860. (e) Kong, L.-W.; Ma, M.-L.; Wu, L.-C.; Zhao, X.-L.; Guo, F.; Jiang, B.; Wen, K. *Dalton Trans.* **2012**, *41*, 5625.

(22) (a) Katz, J. L.; Sellby, K. J.; Conry, R. R. *Org. Lett.* **2005**, *7*, 3505. (b) Ferrini, S.; Fusi, S.; Giorgi, G.; Ponticelli, F. *Eur. J. Org. Chem.* **2008**, 5407. (c) Naseer, M. M.; Wang, D.-X.; Zhao, L.; Huang, Z.-T.; Wang, M.-X. *J. Org. Chem.* **2011**, *76*, 1804.

(23) Mough, S. T.; Holman, K. T. *Chem. Commun.* **2008**, 1407.

(24) (a) Ohmori, O.; Kawano, M.; Fujita, M. *Angew. Chem., Int. Ed.* **2005**, *44*, 1962. (b) Kawano, M.; Kawamichi, T.; Haneda, T.; Kojima, T.; Fujita, M. *J. Am. Chem. Soc.* **2007**, *129*, 15418. (c) Inokuma, Y.; Arai, T.; Fujita, M. *Nat. Chem.* **2010**, *2*, 780. (d) Batten, S. R.; Hoskins, B. F.; Robson, R. *J. Am. Chem. Soc.* **1995**, *117*, 5385. (e) Batten, S. R.; Hoskins, B. F.; Moubaraki, B.; Murray, K. S.; Robson, R. *Chem. Commun.* **2000**, 1095. (f) Dybtsev, D. N.; Chun, H.; Kim, K. *Chem. Commun.* **2004**, 1594. (j) Barrios, L. A.; Ribas, J.; Aromì, G. *Inorg. Chem.* **2007**, *46*, 7154.